

# A Multi-scale Approach for Delineating Individual Tree Crowns with Very High Resolution Imagery

AAG Remote Sensing Specialty Group 2008 Award Winner<sup>1</sup>

Le Wang

## Abstract

*This paper presents a multi-scale approach for delineating individual tree crowns (ITC) from high spatial resolution imagery. By analyzing the evolution of image gradients over the scale-space constructed with orthogonal wavelets, tree crown boundaries are effectively strengthened while the textures resulted from tree branches and twigs are largely suppressed. Two scale consistency checks, a scale and a geometric consistency check, were devised to account for tree crown's radiometric and geometric characteristic. After an edge-enhanced image was acquired, a previously developed marker-controlled watershed segmentation method was adopted to delineate ITC. An experiment was carried out in a study site in California. Field measurements of crown size of 58 trees were compared with those derived from aerial imagery. An R square value of 0.68 was achieved. It was found that crown size was underestimated from the photo interpretation compared to that from the ground survey. The result can be attributed to the fact that pixels lying on the tree crown boundaries are poorly represented in the image.*

## Introduction

A common practice in forest studies is to stratify forests into different stands. Each stand occupies a contiguous area that contains a number of trees that are relatively similar in species composition or age and different from adjacent areas (Lindenmayer and Franklin, 2002). At the stand level, various parameters are of interest including tree density, stand diameter, stand table, stand height, crown closure, stand volume, and site index. Timely and accurate acquisition of these parameters is not only critical to updating forest inventory, which normally deals with the estimation of spatial distribution of wood volume (Spurr, 1948), but is also vital for ecological studies, in which quantitative modeling of ecosystem processes can be made possible with such parameters as inputs (Palace *et al.*, 2008). Compared to traditional labor-intensive field surveys, remote sensing opens up an effective and unique avenue to acquire these parameters in a more automatic fashion. This paper aims at automatically deriving one of these important stand-level parameters, tree crowns, from remote sensing imagery.

The increasing availability of Very-High-Resolution (VHR: one meter or sub-meter level) imagery from either airborne or

satellite optical sensors has boosted the development of automated methods for acquiring the above-mentioned stand-level forest parameters (Wang *et al.*, 2004). In particular, individual tree crowns (ITC) delineations have drawn substantial attention from researchers in the field of remote sensing. Since the 1990s, a number of methods have been developed that utilize spatial, spectral, texture, and contextual characteristics pertinent to the tree crowns in the process of ITC delineations (Gougeon, 1995; Pollock, 1996; Brandtberg and Walter, 1998; Pouliot *et al.*, 2002; Erikson, 2003; Leckie *et al.*, 2003; Wang *et al.*, 2004; Hirschmugl *et al.*, 2007; Palace *et al.*, 2008). Although various extents of successes have been achieved, most of these methods are applied to imagery at a single spatial scale, usually the original scale at which the image was acquired. Since trees naturally occur at different spatial scales, the ultimate solution for the tree crown delineation should be sought from multi-scale analyses, an approach that has similarity with the general practice of human vision system.

In this regard, Brandtberg and Walter (1998) developed a multi-scale method to tackle ITC delineations by adapting the scale-space theory that has been developed in the field of computer vision. Later, Brandtberg *et al.* (2003) applied a similar multi-scale scheme to lidar data in a deciduous forest in eastern US. Scale-space comprises a family of derived signals adopted to represent the original signal at various levels of scale (Lindeberg, 1990). When scale-space methods are applied to a forested image, a series of images is derived with successively coarse features suppressed. For example, tree branches are the major components that are visible at the finest scale but are gradually suppressed at increasing coarse spatial scales. With further coarsening of the scale, tree crowns may be expected to be more apparent before they too become merged into a forest stand at the coarsest scale.

---

<sup>1</sup> In recognition of the 100<sup>th</sup> Anniversary of the Association of American Geographers (AAG) in 2004, the AAG Remote Sensing Specialty Group (RSSG) established a competition to recognize exemplary research scholarship in remote sensing by post-doctoral students and faculty in Geography and allied fields. Dr. Le Wang submitted this paper, which was selected as the 2008 winner.

Hence, when individual trees are of interest, it is not true that the best performance will come from the image with the finest scale because the internal tree structures, such as branches and twigs, will be confused with the boundaries separating tree crowns. This phenomenon in turn raises a serious question: at what scale, or interval of scales, can ITC delineations be tackled most effectively? Given the fact that within a forest stand, tree crowns are likely to have different sizes, it becomes difficult or impossible to choose a single scale based on which all the trees can be identified. Consequently, information at multiple scales should be investigated and effectively integrated in order to produce a more accurate crown delineation.

To this end, this paper presents a multi-scale scheme based on scale-space theory to identify tree crown boundaries while suppressing excessive texture within the tree crown. In an earlier work, Wang *et al.* (2004) developed a marker-controlled watershed segmentation method to solve ITC boundaries and treetop locations at the same time. However, a critical restriction of that method was that it chose a single smoothing scale parameter ( $\sigma$ ) as the basis for executing Laplacian of Gaussian (LOG) edge detection. The proposed multi-scale scheme aims to provide an effective preprocessing method, so that the previously developed method (Wang *et al.*, 2004) can be made more robust and applied to more complex forest scenarios.

## Study Site and Data Preparation

### Study Site

The study site for testing the developed multi-scale scheme is a young ponderosa pine forest stand located at 38°53'42.9"N, 120°37'57.9"W, adjacent to Blodgett Forest Research Station, a research forest of the University of California, Berkeley. In 2000, the stand was dominated by 10 to 11 year old ponderosa pine (*Pinus ponderosa*). The stand has an average diameter at breast height (DBH) of 9.81 cm, an average height (DBH > 3 cm) of 4.05 m, and a density (DBH > 3 cm) of 420 stems/hectare. Over-story leaf area index (LAI) was about 3.2. In May 2000, a pre-commercial thinning took place with a thinning density of 60 percent. Most of shrubs and grass are cut down. The thinning and removal of shrubs and grasses improves the spatial separation of the trees in the image, and the contrast between the trees and background.

### Data Preparation

A set of 1:8 000 aerial photographs was acquired by an aerial camera with a focal length of 152.9 mm and color aerial film in May 2000 under conditions of uniform cloud covering the study area. The uniform cloud condition helps alleviate shadow problems, and therefore, eases the process of tree crown delineation. After the aerial photos were developed, they were scanned at 1,000 dpi resulting in an effective spatial resolution approximately 20.3 cm on the ground. A sub-area of 500 × 500 pixels was chosen as the study area, corresponding to a ground area of 10,404 m<sup>2</sup> (Figure 1).

A total of 58 trees was selected in a subset of the study area, as they have been labeled for conducting a long-term carbon study. They were measured on the ground on the same day as the aerial photography was acquired. The tree crown diameter was measured in two directions. One measurement was made along the maximum axis of the tree crown. Then, the second measurement was made along the perpendicular direction to the first one. The two measurements were averaged to generate a radius value for each ITC. The tree boles' perimeter at the height of 1.35 m was measured to derive the tree DBH. The 58 trees were identified on the aerial

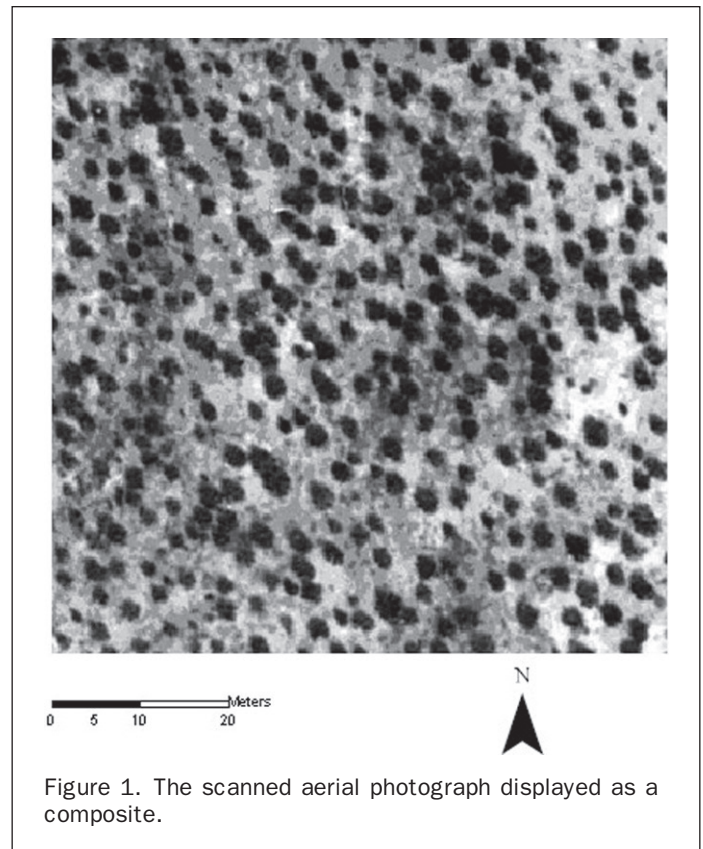


Figure 1. The scanned aerial photograph displayed as a composite.

photos, and a one-to-one correspondence was made for trees between photograph and field measurements.

## Methods

### Scale-space Theory

Scale-space theory aims at making significant structures and scales explicit (Lindeberg, 1993). The idea is to link low level features detected at different scales in scale-space, thus facilitating the identification of high level objects (Lu and Jain, 1992). The scale-space is also termed an image pyramid. Differing in how to construct scale-space or how to decompose the original image into pyramids, there are two major categories of scale-space, i.e., linear and non-linear.

### Linear Scale-space

Linear scale-space was proposed by Witkin (1983). He embedded the original image in a one parameter family of derived images, the scale-space, where the parameter  $t$  describes the current level of scale resolution. Specifically with this method, the image pyramid is constructed by successively convolving the original image with a lowpass filter. The resulted scale-space has to follow a strict rule: when the scale parameter  $t$  is increased, additional local extrema or additional zero crossings cannot appear. Babaud *et al.* (1986) proved that the Gaussian filter is the only kernel that satisfies the above-mentioned rule for 1D signal. Yuille and Poggio (1986) extended this proof to 2D signal in demonstrating that zero crossings of linear derivative have this scaling behavior, if and only if the image is filtered by a 2D rotationally symmetric Gaussian. In this case, the scale  $t$  is specifically determined by the  $\sigma$  of the Gaussian filter.

By increasing the  $\sigma$  value of Gaussian filter and convolving it with the original image, a Gaussian pyramid is

obtained. The difference of any two consecutive scale images gives an approximation of the Laplacian of Gaussian. In this manner, a Laplacian pyramid is generated as well. Burt and Adelson (1983) and Crowley (1987) separately implemented the proposed Laplacian pyramid and found two inherent problems when successive convolution was used to construct the scale-space. First, correlation exists among different level of images in the Laplacian pyramid, and it prevents differentiating true image details from the intrinsic redundancy of the representation. Second, the Laplacian pyramid does not contain the spatial orientation information, a property that is inconvenient for object recognition problems.

Mallat (1989) provides a wavelet-based decomposition scheme to build the linear scale-space, i.e., a wavelet representation. By definition, a function  $\theta(x)$  is called a scaling function if the following criterion is met:

$$\int_{-\infty}^{\infty} \theta(x) dx = 1. \text{ A function } \psi(x) \text{ can be called a wavelet if}$$

the following criterion is met:  $\int_{-\infty}^{+\infty} \psi(x) dx = 0$ . Wavelets are

also referred to as “mother functions.” By successively convolving the original image with a dilated and transformed scaling function, approximations of the image at all the intermediate scales are obtained. To be named as a multi-resolution approximation, the scaling function cannot be chosen arbitrarily, but has to satisfy seven criteria listed by Mallat (1989). By convolving the original image with the dilated and transformed wavelet, the difference between any two approximations is extracted. Consequently, the original image can be decomposed as one approximation image together with various difference images at different scales. Given that only a limited range of scales can be chosen for the decomposition, Mallat and Zhong (1992) proposed a dyadic wavelet transform in which the scale varies only along the dyadic sequence ( $2^j$ ). They proved that although the image was decomposed only at the dyadic scales, it can be fully recovered with the summation of approximations and differences that were acquired during the decomposition.

Compared to the Laplacian pyramid, the wavelet decomposition has several strengths: first, no correlation exists among different levels due to the decomposition of the original image (the independence is due to the orthogonality of the wavelet functions); second, it is possible to characterize local edges based on coefficients in a wavelet orthonormal basis expansion (the spatial orientation of edges can be differentiated in a wavelet decomposition); third, orthonormal wavelets have good localization properties in both the spatial and Fourier domain.

#### Non-linear Scale-space

The second category of methods for constructing a scale-space is through non-linear operators. Pei and Chen (1995) proposed a non-redundant decomposition scheme based on mathematical morphology. However, their method cannot guarantee a complete reconstruction. Egger and Li (1995) developed a non-linear decomposition scheme with perfect reconstruction based on a median-type operator. Although non-linear scale-space provides some intriguing characteristic features that cannot be obtained in linear scale-space, non-linear decomposition has received less attention compared to its linear counterparts due to some unresolved theoretical problem (Borsworth and Acton, 2003).

#### A Wavelet-based Method to Enhance Tree Crown Boundaries

In this study, a multi-scale scheme was developed with use of wavelet methods. Scharcanski *et al.* (2002) proposed a

denoising method based on wavelet decomposition. I revised and adapted their methods for enhancing tree crown boundaries instead of denoising. First, an orthonormal wavelet basis was used to construct a linear scale-space through which image edges were carefully examined at series of scales. By exploring the evolution of the edges, I discriminated edges that correspond to true tree crown boundaries from edges that correspond to the tree branches and twigs. Then, the image texture within a single tree crown was suppressed while true edge boundaries were strengthened. A systematic framework of the scheme is presented in Figure 2. The following sections provide the details for each step.

#### Dyadic Wavelet Decomposition

I adopted the cubic spline function that was used in Mallat (1989) as the scaling function for the multi-resolution representation. The scaling function can be treated as a low-pass smoothing filter. In turn, the wavelet function can be considered as the derivative of the smoothing function with orthonormal characteristics. In the discrete wavelet transform, calculating wavelet coefficients at every possible scale requires an impractical amount of work. Thus, the dyadic wavelet decomposition was applied in this study, i.e., only scales at the power of 2 were used. At each decomposed level, four wavelet coefficients were obtained: approximate, horizontal, vertical, and diagonal coefficients. Mallat and Zhong (1992) found one can obtain a precise description of the signal sharp variation points from the evolution of the wavelet transform modulus maxima across scales. Since the objective of using wavelet decomposition is to quantify the evolution of different sources of edge pixels across the scale-space, the gradient magnitude and orientation was calculated at the scale  $2^j$  with Equations 1 and 2.

$$M_{edge} = \sqrt{(W_{2^j}^h)^2 + (W_{2^j}^v)^2} \quad (1)$$

$$A_{edge} = \arctan\left(\frac{W_{2^j}^v}{W_{2^j}^h}\right) \quad (2)$$

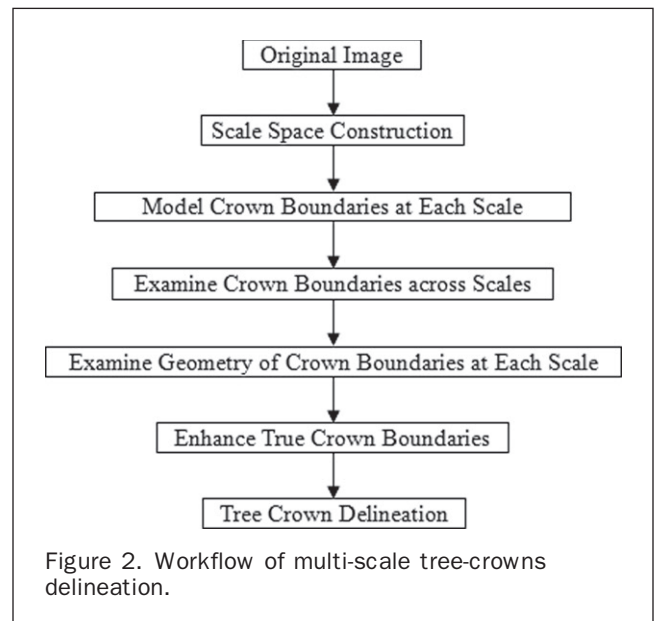


Figure 2. Workflow of multi-scale tree-crowns delineation.

where  $M_{edge}$  stands for gradient magnitude,  $W_{2^j}^h$  and  $W_{2^j}^v$  are the wavelet coefficients for horizontal and vertical directions, respectively, and  $A_{edge}$  stands for the gradient orientation.

#### Edge Probability by Modeling the Gradient Magnitude

Although an edge magnitude was obtained at each scale for every pixel, using a simple threshold to judge whether a specific pixel belongs to edge or the background apparently cannot work effectively on a complex forest image. On the other hand, edge probability provides a more accurate way to tell edge pixels apart from background pixels than a simple threshold method. Scharcanski *et al.* (2002) showed the gradient magnitude of background related pixels can be modeled by a Rayleigh probability density function as follows,

$$P_j(r/background) = \frac{r}{[\sigma_{background}^j]^2} \exp^{-r^2/2[\sigma_{background}^j]^2} \quad (3)$$

in which:  $P_j(r/background)$  is the probability of a pixel having gradient magnitude equal to  $r$ , given that it belongs to a background pixel at the scale of  $2^j$ , and  $\sigma_{background}^j$  is the standard deviation of a background pixel's gradient magnitude at the scale of  $2^j$ . Here background can be understood as the pixels falling within tree crowns but not on the boundaries of tree crowns.

In the same manner, the gradient magnitude of edge-related pixels can be modeled by the same form of Rayleigh probability density function with a new  $\sigma$  value that corresponds to edge pixels instead of background ones. The equation is as follows:

$$P_j(r/edge) = \frac{r}{[\sigma_{edge}^j]^2} \exp^{-r^2/2[\sigma_{edge}^j]^2} \quad (4)$$

As a result of the Equations 3 and 4, the overall probability of a pixel occupying the gradient magnitude value equal to  $r$  is given by:

$$P_j(r) = w_{background}^j P_j(r/background) + (1 - w_{background}^j) P_j(r/edge) \quad (5)$$

By associating Equation 5 with Equations 3 and 4, it can be observed that three parameters have to be known in order to calculate  $P_j(r)$ . They are  $w_{background}^j$ ,  $\sigma_{edge}^j$ , and  $\sigma_{background}^j$ . In the field of computer science, a typical method to solve the three unknown parameters is through maximizing the likelihood function as follows:

$$[w_{background}^j, \sigma_{edge}^j, \sigma_{background}^j] = \arg \max(\prod p_j(r)) \quad (6)$$

in which:  $\prod p_j(r)$  stands for the joint probability of gradient magnitude, while  $w_{background}^j$  is the prior probability of a pixel being background or noise.

By respectively modeling the distribution of magnitude for the two types of pixels (edge and background), I end up with using the Bayes theorem to calculate a posterior probability  $p(edge/r)$  as described in Equation 7:

$$p(edge/r) = \frac{(1 - w_{background}^j) p(r/edge)}{p(r)} \quad (7)$$

where  $p(edge/r)$  stands for the probability of a pixel belonging to edge given the gradient magnitude is equal to  $r$ .

As a result of the calculation of  $p(edge/r)$ , I assigned a probability to every pixel to quantify its similarity to an edge pixel. The probability  $p(edge/r)$  will take the place of gradient magnitude in the following process to enhance tree crown boundaries.

#### Scale Consistency Constraints

Solely using the gradient magnitude or the probability of edge at a single scale, it is very hard to differentiate true crown boundaries from the small textures embedded within a tree crown, for example, twigs and branches. Since scale-space provides a range of scales, it is now possible to monitor the evolution of each pixel along various scales, from which the expected discrimination goal can be achieved. A basic assumption is made that in the scale-space, true crown boundaries will demonstrate a consistently large edge probability whereas undesired texture pixels will only possess a large edge probability at a specific or a small range of scales. To accomplish this goal, I chose the calculation of harmonic mean to evaluate the scale consistency as follows:

$$p_j(edge/r) = \frac{M+1}{\frac{1}{p_j(edge/r)} + \frac{1}{p_{j+1}(edge/r)} + \dots + \frac{1}{p_{j+m}(edge/r)}} \quad (8)$$

in which  $p_j(edge/r)$  is the edge probability at the scale  $2^j$ ,  $p_{j+m}(edge/r)$  is the edge probability at the scale  $2^{j+m}$ , and  $M+1$  is the total number of scales that are included in the analysis.

The harmonic mean of edge probability at  $M+1$  scales will be used to update edge probability at the current scale  $2^j$ . In this way, a true crown boundary pixel's edge probability will be further enhanced and the undesired small texture's edge probability will be suppressed because they only demonstrate an inconsistent edge probability.

#### Geometric Consistency Constraints

Given that the tree crowns are usually curved in shape, the gradient orientation along the pixels in the same tree crown boundary should not undergo significant changes, but instead should follow a smooth transition. Using Equation 2, I assigned each pixel with a gradient direction. The gradient direction of current pixel indicates the next step to which tree crown should extend in the 8-neighborhood. Figure 3 presents a typical example of a

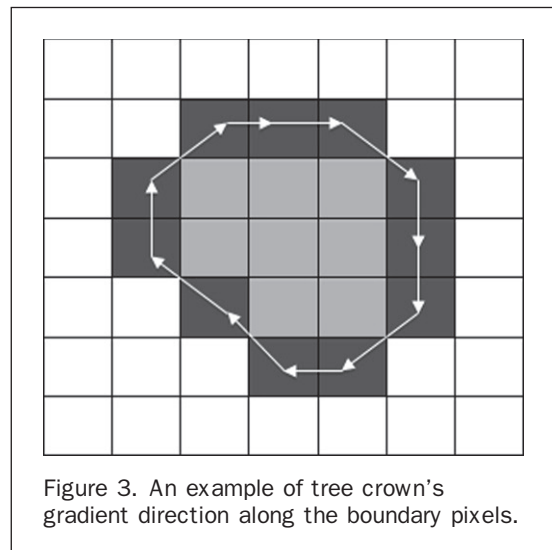


Figure 3. An example of tree crown's gradient direction along the boundary pixels.

tree crown with the gradient direction represented with the arrow for the boundary pixels.

In theory, the calculated gradient direction can take any possible value between 0 and 180 degrees. For simplicity, I first quantize the gradient direction into eight groups of directions: 0°, 22.5°, 45°, 67.5°, 90°, 112.5°, 135°, and 157.5°. Then, I obtained a new edge probability  $p_i(\text{edge}/r)$  by accumulating the existing probability along the gradient direction with the weight assigned by a Gaussian function. The following is an example of the weights adopted when the gradient direction for current pixel is 45° and 0°, respectively (Table 1).

The geometric consistency will strengthen edge pixels along a continuous smooth curve, whereas the isolated edge pixels will be suppressed. Given the fact that small texture pixels in a tree crown tend to generate isolated edge pixels, the geometric consistency strengthens the edge probability along the true crown boundary.

Up to this point, I have conducted two-consistency constraints (scale and geometric consistency constraints) along the scale-space that was constructed by wavelet decomposition. The consistency constraints are designed with a purpose to augment the ITC boundary from various sources of edges. As a result of the consistency check, an enhanced edge probability at any dyadic scales was derived.

#### Inverse Wavelet Transform

To integrate the enhancement that was obtained at different scales, the wavelet coefficients (horizontal and vertical ones) were modified according to the acquired edge probability. Together with the same approximation and diagonal coefficients derived from the decomposition step, an inverse wavelet transformation was applied to reconstruct the image with the crown boundary strengthened using the same scaling function.

#### Tree Crowns Delineation with Marker-controlled Watershed Segmentation

With the enhanced version of the tree image, task of delineating the tree crown boundary now becomes much easier because the undesired texture has been largely reduced. The marker-controlled watershed segmentation method introduced in Wang *et al.* (2004) was adopted using the edge enhanced tree image.

#### Experiment Results and Discussion

With the aerial photos, I first undertook an object-based classification using eCognition® 4.0 software with a classification scheme containing two classes: tree crown pixels and background pixels. The classification allowed removing the

noise coming from the bare soil and other undesired features. As a result, I assigned a zero value to those pixels that were classified as background pixels while still kept the original tonal information for the tree crown pixels. Next, the filtered color image was transformed to a grey level image through an Intensity-Hue-Saturation transformation. Only the intensity image was used in the subsequent processing, because the tree crown delineation method can only handle grey level images.

As previously described, dyadic wavelet decomposition was implemented, and I chose the decomposition level as 3 as it is more computationally efficient. Consequently, the coefficients for the approximation and details at each level were derived, and the gradient magnitude and gradient direction was calculated. The histograms of gradient magnitudes at the scale  $2^1$ ,  $2^2$ ,  $2^3$  are presented in Figure 4.

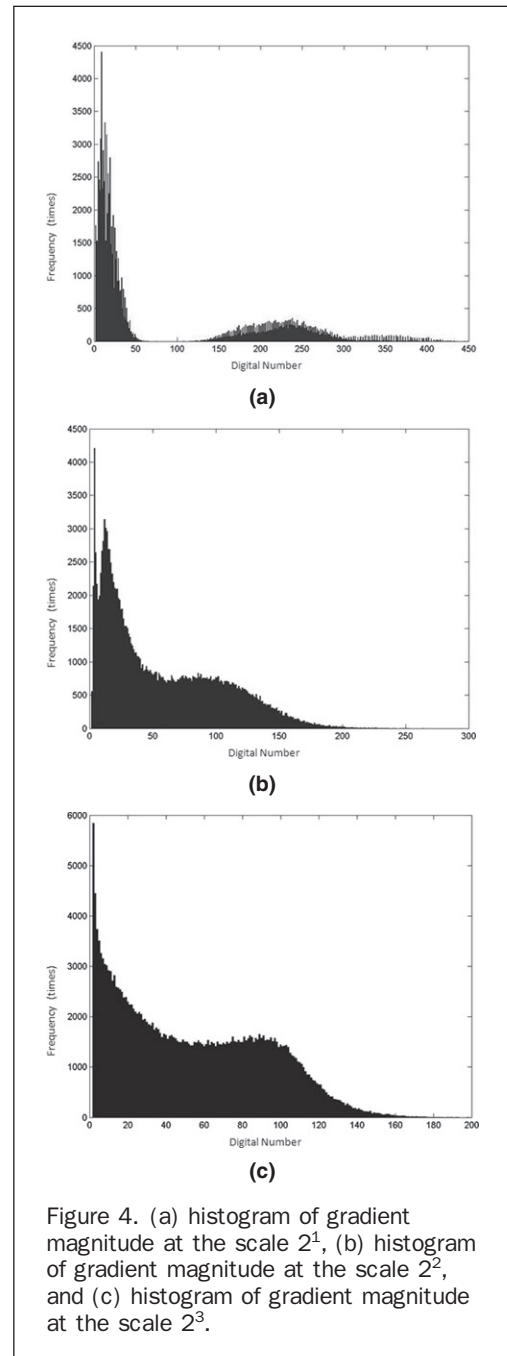


Figure 4. (a) histogram of gradient magnitude at the scale  $2^1$ , (b) histogram of gradient magnitude at the scale  $2^2$ , and (c) histogram of gradient magnitude at the scale  $2^3$ .

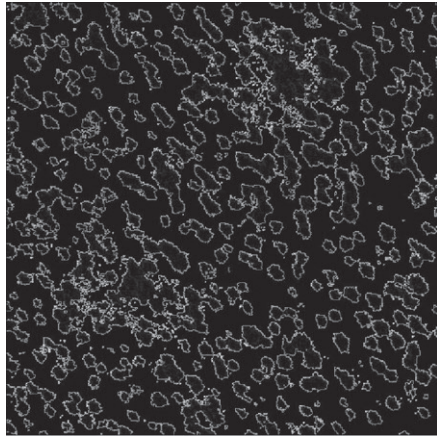
TABLE 1. WEIGHT FUNCTION USED IN GEOMETRIC CONSISTENCY CHECK: (A) WEIGHT FUNCTION WHEN GRADIENT DIRECTION = 45°, AND (B) WEIGHT FUNCTION WHEN GRADIENT DIRECTION = 0°

0	0	0	0	0	0	0.1186
0	0	0	0	0	0.1418	0
0	0	0	0	0.1578	0	0
0	0	0	0.1636	0	0	0
0	0	0.1578	0	0	0	0
0	0.1418	0	0	0	0	0
0.1186	0	0	0	0	0	0

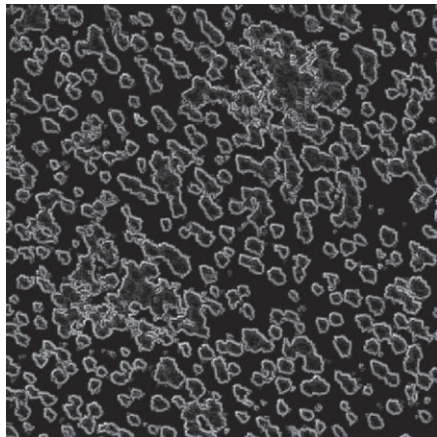
(A)

0.1186	0.1418	0.1578	0.1636	0.1578	0.1418	0.1186
--------	--------	--------	--------	--------	--------	--------

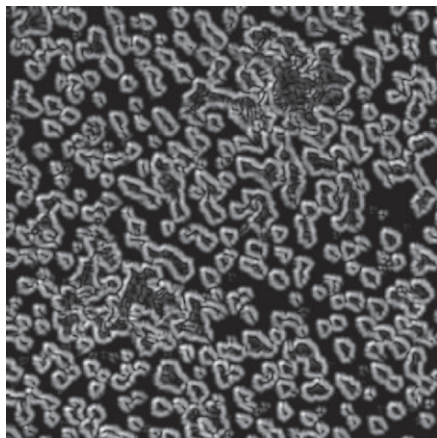
(B)



(a)



(b)



(c)

Figure 5. (a) Edge probabilities at the scale  $2^1$ , (b) Edge probabilities at the scale  $2^2$ , and (c) Edge probabilities at the scale  $2^3$ .

It is easy to observe the bi-modal shape in the histograms, which motivates me to model true crown boundary and other background separately. Subsequently, Figure 5 exhibited the edge probability that was calculated according to the Equation 7 at the scale  $2^1$ ,  $2^2$ ,  $2^3$ , respectively.

Furthermore, the scale consistency was conducted based on the calculation of harmonic mean, and the geometric consistency was accomplished through the use of gradient consistency. An updated edge probability was applied to adjust the magnitude of the horizontal and vertical wavelet coefficients based on which an inverse wavelet transform was carried out.

The resulting image is presented in Figure 6. To illustrate the effect of wavelet enhanced method, the post-enhanced version of the image was subtracted from the original image, and a shaded relief image is laid out in Figure 7 to show the difference between the two images. As can be seen from Figure 7, a significant number of small textures within tree crowns stand out in the difference image, suggesting they have been suppressed on the enhanced image. This result largely alleviates the difficulty for using edge detection method to extract tree crown boundary in the subsequent steps.

The tree crown delineation method that was introduced in Wang *et al.* (2004) was then applied to the enhanced version of the image. The gradient was chosen as the watershed function based on which marker-controlled watershed segmentation was executed. Final delineated tree crowns are shown in the Figure 8. As a further step to make the results usable for Geographic Information System (GIS) applications, a conversion was carried out to transform the tree crowns to a polygon coverage that can be easily imported into many popular GIS packages, for example, ESRI's ArcView<sup>®</sup> software.

As a further validation, for the total of 58 trees measured from the ground, 56 trees were correctly identified from the automated method. Two trees were missing from the automated method. For the 56 correctly-identified trees, crown size was then compared between the automated method and the field measurements. The crown area was directly extracted by using the function embedded in ArcView<sup>®</sup>. The area was then converted to the radius based on a circular crown shape assumption. The automated and

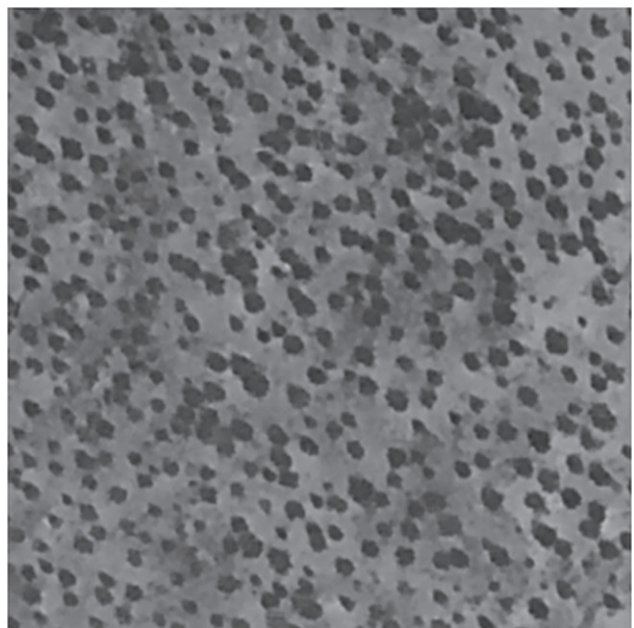


Figure 6. Enhanced image from the inverse wavelet transform.

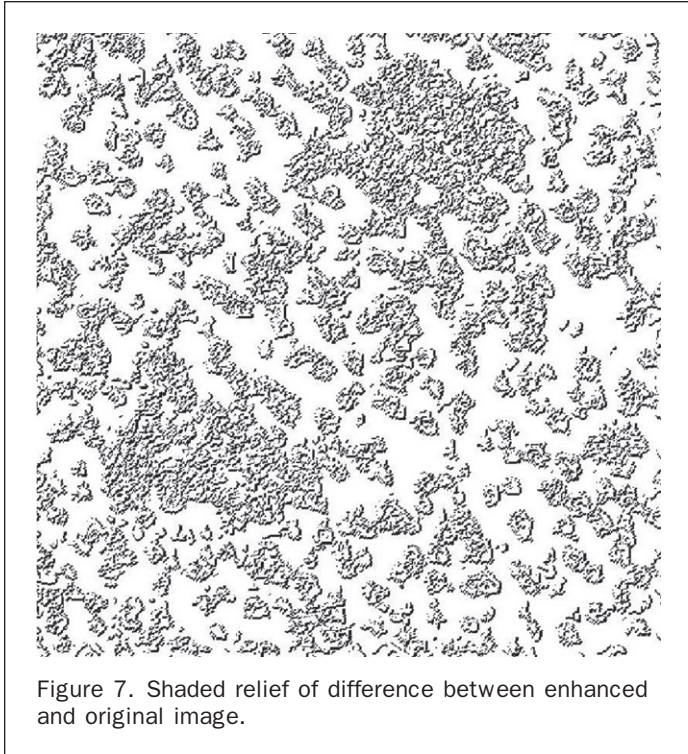


Figure 7. Shaded relief of difference between enhanced and original image.

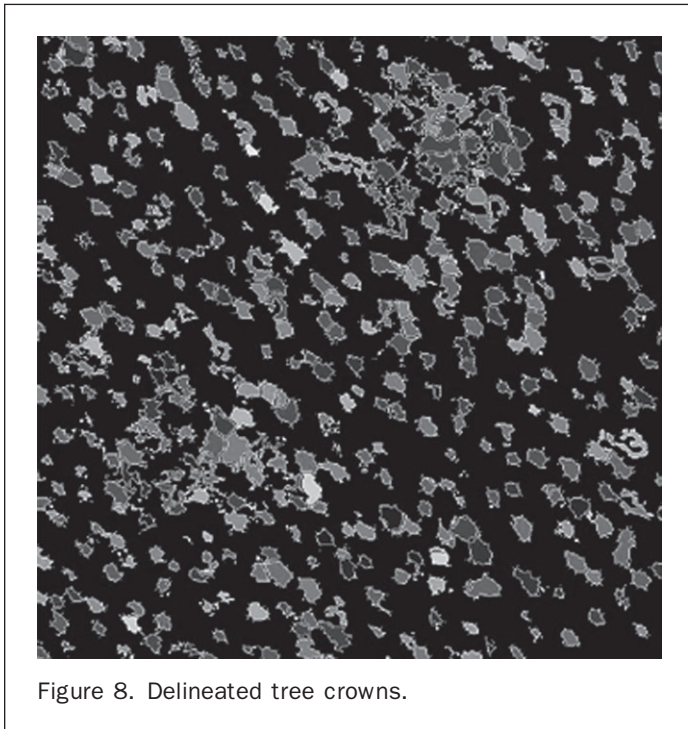


Figure 8. Delineated tree crowns.

field measurements were then regressed (Figure 9). It is worthwhile to point out that noise is introduced when a circular shape was used to convert the irregular crown area to radius value. The noise partly contributes to the relative low  $r^2$  (0.68). The slope value in the regression equation is 0.875, indicating that crown size was underestimated from the photo interpretation. The result can be attributed to the

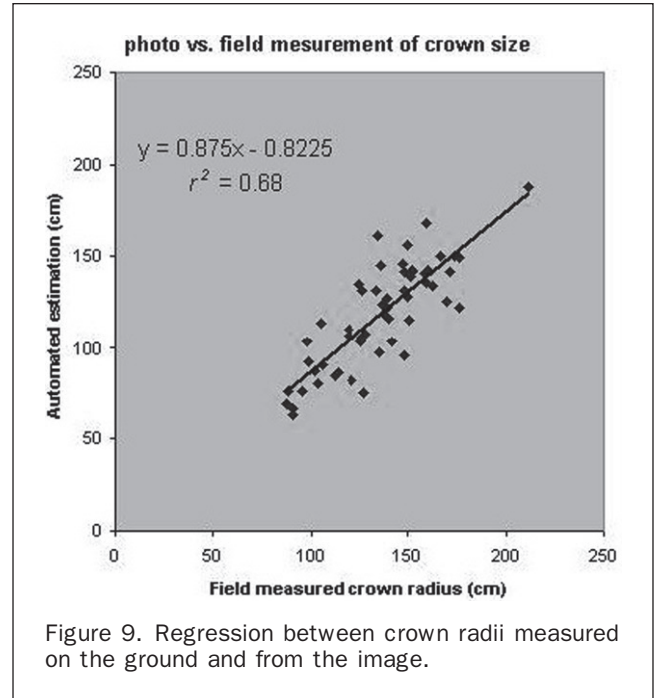


Figure 9. Regression between crown radii measured on the ground and from the image.

fact that pixels lying on the tree crown boundaries are not well recorded in the image.

## Conclusions

In summary, by analyzing the evolution of image gradients over the scale-space that was constructed based on orthogonal wavelets, tree crown boundaries are effectively strengthened while the textures resulted from tree branches and twigs are largely suppressed. The scale and geometric consistency check play an important role in the process of enhancement because they account for tree crown's characteristic in terms of both radiance and shape. Promising ITC delineations were achieved with the developed multi-scale scheme. 56 out of 58 field-surveyed trees were identified from the automated method. A comparison of crown size for 56 trees were conducted between those derived from aerial image and those measured on the ground. R square value of 0.68 was achieved indicating the feasibility of obtaining crown area from remote sensing imagery. In addition, it was found that crown size was underestimated from the photo interpretation compared to that from the ground survey. In practice, for a VHR image, it is necessary to perform an effective enhancement before the tree crown delineation can be employed. In future work, this developed method should be tested in a range of forests, most importantly in undisturbed forest that has not been thinned. Adoption of different types of imagery, such as the latest high spatial resolution satellite imagery, may help to further augment the agreement of image-derived crown size in relation to ground truth.

## Acknowledgments

The study was partly supported by grants to Le Wang from the National Science Foundation (DEB-0810933 and BCS-0822489). The author thanks Professors Peng Gong and Gregory Biging at University of California at Berkeley for their generous support for acquiring the remote sensing data.

## References

- Babaud, J., A.P. Witkin, M. Baudin, and R.O. Duda, 1986. Uniqueness of the Gaussian Kernel for scale-space filtering, *IEEE Transactions on Pattern Analysis and Machine Intelligence*, 8:26–33.
- Borworth, J.H. and S.T. Acton, 2003. Morphological scale-space in image processing, *Digital Signal Processing*, 13:338–367.
- Brandtberg, T., and F. Walter, 1998. Automated delineation of individual tree crowns in high spatial resolution aerial images by multiple-scale analysis, *Machine Vision and Applications*, 11:64–73.
- Brandtberg, T., T.A. Warner, R.E. Landenberger, and J.B. McGraw, 2003. Detection and analysis of individual leaf-off tree crowns in small footprint, high sampling density lidar data from the eastern deciduous forest in North America, *Remote Sensing of Environment*, 85(3):290–303.
- Burt, P.J., and E.H. Adelson, 1983. The Laplacian Pyramid as a compact image code, *IEEE Transactions on Communications*, 31:532–540.
- Crowley, J., 1987. A representation for visual information, *Robotic Institute, Carnegie-Mellon University Technical Report CMU-RI-TR-82-7*.
- Egger, O., and W. Li, 1995. Very low bit rate image coding using morphological operators and adaptive decompositions, *Proceedings of the IEEE International Conference on Image Processing*, Austin, Texas, pp. 272–287.
- Erikson, M., 2003. Segmentation of individual tree crowns in colour aerial photographs using region growing supported by fuzzy rules, *Canadian Journal of Forest Research-Revue Canadienne De Recherche Forestiere*, 33:1557–1563.
- Gougeon, F.A., 1995. A crown-following approach to the automatic delineation of individual tree crown in high spatial resolution aerial images, *Canadian Journal of Remote Sensing*, 21:274–284.
- Hirschmugl, M., M. Ofner, J. Raggam, and M. Schardt, 2007. Single tree detection in very high resolution remote sensing data, *Remote Sensing of Environment*, 110:533–544.
- Leckie, D.G., F.A. Gougeon, N. Walsworth, and D. Paradine, 2003. Stand delineation and composition estimation using semi-automated individual tree crown analysis, *Remote Sensing of Environment*, 85:355–369.
- Lindeberg, T., 1990. Scale-space for discrete signals, *IEEE Transactions on Pattern Analysis and Machine Intelligence*, 12:234–254.
- Lindeberg, T., 1993. Detecting salient blob-like image structures and their scales with a scale-space primal sketch - A method for focus-of-attention, *International Journal of Computer Vision*, 11:283–318.
- Lindenmayer, D.B., and J.F. Franklin, 2002. *Conserving Forest Biodiversity: A Comprehensive Multiscaled Approach*, Island Press, Washington, D.C., 351 p.
- Lu, Y., and R.C. Jain, 1992. Reasoning about edges in scale-space, *IEEE Transactions on Pattern Analysis and Machine Intelligence*, 14:450–468.
- Mallat, S., and S. Zhong, 1992. Characterization of signals from multiscale edges, *IEEE Transactions on Pattern Analysis and Machine Intelligence*, 14:710–732.
- Mallat, S.G., 1989. A theory for multiresolution signal decomposition - The wavelet Representation, *IEEE Transactions on Pattern Analysis and Machine Intelligence*, 11:674–693.
- Palace, M., M. Keller, G.P. Asner, S. Hagen, and B. Braswell, 2008. Amazon forest structure from IKONOS satellite data and the automated characterization of forest canopy properties, *Biotropica*, 40:141–150.
- Pei, S.C., and F.C. Chen, 1995. Hierarchical image representation by mathematical morphology subband decomposition, *Pattern Recognition Letters*, 16:183–192.
- Pollock, R., 1996. The automatic recognition of individual trees in aerial images of forests based on a synthetic tree crown image model, *Department of Computer Science*, Vancouver, Canada, University of British Columbia, p. 158.
- Pouliot, D.A., D.J. King, F.W. Bell, and D.G. Pitt, 2002. Automated tree crown detection and delineation in high-resolution digital camera imagery of coniferous forest regeneration, *Remote Sensing of Environment*, 82:322–334.
- Scharcanski, J., C.R. Jung, and R.T. Clarke, 2002. Adaptive image denoising using scale and space consistency, *IEEE Transactions on Image Processing*, 11:1092–1101.
- Spurr, S.H., 1948. *Aerial Photographs in Forestry*, New York, Ronald Press Company.
- Wang, L., P. Gong, and G.S. Biging, 2004. Individual tree-crown delineation and treetop detection high-spatial-resolution aerial imagery, *Photogrammetric Engineering & Remote Sensing*, 70(3):351–357.
- Witkin, A.P., 1983. Scale-space filtering, *Proceedings of the 8<sup>th</sup> International Joint Conference on Artificial Intelligence*, pp. 1019–1022.
- Yuille, A.L., and T.A. Poggio, 1986. Scaling theorems for zero crossings, *IEEE Transactions on Pattern Analysis and Machine Intelligence*, 8:15–25.